



Research Paper

Analysis of Somatic Mutations in Senescent Cells Using Single-Cell Whole-Genome Sequencing

Lei Zhang,^{1,2} Marco De Cecco,³ Moonsook Lee,⁴ Xiaoxiao Hao,⁴ Alexander Y. Maslov,^{4,5} Cristina Montagna,⁶ Judith Campisi,^{7,8} Xiao Dong,^{1,9,*} John M. Sedivy,^{3,*} and Jan Vijg^{4,10,*}

¹Institute on the Biology of Aging and Metabolism, University of Minnesota, Minneapolis, MN, USA

²Department of Biochemistry, Molecular Biology and Biophysics, University of Minnesota, Minneapolis, MN, USA

³Department of Molecular Biology, Cell Biology and Biochemistry, and Center on the Biology of Aging, Brown University, Providence, RI, USA

⁴Department of Genetics, Albert Einstein College of Medicine, Bronx, NY, USA

⁵Laboratory of Applied Genomic Technologies, Voronezh State University of Engineering Technology, Voronezh, Russia

⁶Department of Radiation Oncology, Rutgers Cancer Institute of New Jersey, New Brunswick, NJ, USA

⁷Buck Institute for Research on Aging, Novato, CA, USA

⁸Lawrence Berkeley National Laboratory, Berkeley, CA, USA

⁹Department of Genetics, Cell Biology and Development, University of Minnesota, Minneapolis, MN, USA

¹⁰Center for Single-Cell Omics, School of Public Health, Shanghai Jiao Tong University School of Medicine, Shanghai, China

*Corresponding authors: dong0265@umn.edu; john_sedivy@brown.edu; jan.vijg@einsteinmed.org

<https://doi.org/10.59368/agingbio.20230005>

Somatic mutations accumulate in multiple organs and tissues during aging and are a known cause of cancer. Cellular senescence is a possible cause of functional decline in aging, yet also acts as an anti-cancer mechanism *in vivo*. Here, we compared somatic mutation burden between early passage and deeply senescent human fibroblasts using single-cell whole-genome sequencing. The results show that single-nucleotide variants (SNVs) and small insertions and deletions (INDELs) are increased in senescent cells by about twofold but have the same mutational signature as early passage cells. The increase in SNVs and INDELs can be explained by increased replication errors due to the increased number of cell divisions senescent cells are likely to have undergone. By contrast, a stark increase of aneuploidies was observed in deeply senescent cells, with about half of all senescent cells affected but none of the early passage cells analyzed. These results indicate that large chromosomal events rather than small base substitutions or insertions and deletions could be mechanistically linked to cellular senescence.

Introduction

Lifelong accumulation of mutations in somatic cells has been implicated as a driver of cancer and aging soon after the discovery of the structure of DNA^{1,2}. Somatic mutations have been detected in clonal cell lineages, such as in cancer, but in the absence of a selective advantage, their random nature and low abundance have stymied accurate detection during aging. With the advent of single-cell whole-genome DNA sequencing, methods for the quantitative analysis of somatic mutations could be developed and have subsequently been widely used to accurately document and quantify such mutations in multiple tissues and cell types during human aging^{3–7}.

Cellular senescence is a cell fate elicited by a variety of stresses and characterized by an essentially irreversible arrest of proliferation⁸. Irreparable DNA damages caused by telomere shortening or replication fork collapse due to oncogene activation are well-studied triggers, and in such contexts, senescence has a beneficial role as a tumor suppression mechanism. Senescent cells, however, also accumulate sporadically in most tissues with aging, where they exert a strong proinflammatory effect⁹ and are believed to promote

many age-related pathologies and diseases¹⁰. Senescence is a complex state that includes widespread gene expression and epigenetic changes¹¹, mitochondrial dysfunction, elevated reactive oxygen species (ROS)¹², persistent DNA double-strand breaks (DSBs), and DNA damage response signaling¹³.

Little is known about the pattern and role of somatic mutations during cellular senescence. On the one hand, given the evidence of increased ROS and DSBs, one might expect accelerated mutation rates in senescent cells; on the other hand, it is reasonable to hypothesize limited mutagenesis given that senescence is a major anticancer mechanism that prevents subsequent cell proliferation¹⁴. To test these conflicting hypotheses, we performed single-cell whole-genome sequencing of early passage and senescent normal human lung fibroblasts and compared the frequencies and spectra of three types of mutations: single-nucleotide variants (SNVs), small insertions and deletions (INDELs), and chromosomal aneuploidies. The results indicate that only aneuploidies occur at a frequency much higher than expected based on the increased number of cell divisions senescent cells are likely to have undergone as compared to early passage cells.

Results

Single-cell whole-genome sequencing of deeply senescent cells and controls

We generated replicatively senescent cells by continuous passaging of the IMR-90 normal human fibroblast cell strain. To allow ample time for other mutagenic events to accumulate, we maintained the senescent cultures for 4–5 months (hereafter referred to as deep senescence). Single cells were isolated from both early passage and deeply senescent cells using the CellRaft System (Cell Microsystems) and amplified using the single-cell multiple displacement amplification (SCMDA) procedure developed previously¹⁵. We performed whole-genome sequencing (average depth of 24×; Table S1) of early passage and deeply senescent single-cell amplicons. We also sequenced bulk DNA from early passage cells, which we used to filter out germline polymorphisms (Fig. 1). Somatic SNVs, INDELS, and aneuploidies were identified from each single cell using the SCcaller and SCCNV pipelines developed previously^{15,16}. Frequencies of SNVs and INDELS per cell were estimated after correcting for genome coverage and sensitivity in variant calling (Table S2)⁷.

Elevated frequencies of SNVs and INDELS in senescent cells

We observed a median of 1103 SNVs per cell in early passage and 2618 SNVs per cell in deeply senescent cells ($p = 0.0022$, Wilcoxon Rank Sum Test, two-tailed; Fig. 2A), reflecting a 2.4-fold higher SNV frequency in senescence. Of note, the frequency of 2618 SNVs per cell is somewhat less but close to the 3127 SNVs per cell we reported in primary B lymphocytes in human centenarians⁷. For INDELS, we also observed significantly higher frequencies in senescent cells as compared to early passage cells (median frequencies of 311 and 165 per cell type, respectively; 1.9-fold; $p = 0.0128$, Wilcoxon Rank Sum Test, two-tailed; Fig. 2B). This was also true for insertions and deletions separately, with the numbers of deletions slightly higher than the numbers of insertions (Supplementary Figure 1A,B). A higher load of SNVs and INDELS in senescent cells is expected

simply based on the additional number of cell divisions undergone by senescent cells, providing more opportunity for SNVs and INDELS as replication errors¹⁷.

Next, we compared mutation spectra of early passage and senescent cells. For SNVs, we observed no significant differences in the fraction of all six SNV types between the two conditions (Fig. 2C). The highest fraction of mutations was that of CG>AT transversions, followed by CG>TA and AT>GC transitions. This similarity between early passage and senescent cells remained when considering the bases flanking the mutations (Fig. 2D,E). For INDELS, we also observed no significant differences: Deletions were 54% of all INDELS, with the remainder being insertions under both conditions (Fig. 2F). By contrast, particular SNV and/or INDEL signatures are often found in tumor cells¹⁸.

We then analyzed the genomic distribution of SNVs and INDELS. Plotting the density of mutations in early passage and senescent cells across the genome to identify possible mutational hotspots, using the R package “karyoploteR”¹⁹, did not reveal any significant chromosomal positional enrichment of mutations (Supplementary Figure 2A,B), which is often found in tumor cells²⁰. This finding was confirmed using the mutation showers algorithm with the R package “ClusteredMutations”^{20,21}, which found no obvious mutational hotspots. Overall, the high similarities in SNV and INDEL spectra and chromosomal distributions between early passage and senescent cells indicate the absence of specific mechanisms for generating SNVs and INDELS in senescent human fibroblasts.

In cancer as well as aging of the hematopoietic system, clonal development of somatic cell lineages has often been observed and associated with health status of human subjects^{22,23}. To test if clonal development can occur during passaging to replicative senescence, we compared the frequencies of overlapping mutations found in two or more cells. Because the mutation frequencies in these cells are not very high, an overlapping mutation found in two cells is unlikely to arise by two independent events, and much more likely the result of a mutation occurring in a progenitor cell. We found 4.6% of mutations in early passage cells occurring in more than one cell, and 10.8% in senescent cells ($p < 2.2 \times 10^{-16}$, chi-squared test, two-tailed). This 2.4-fold increase suggests an

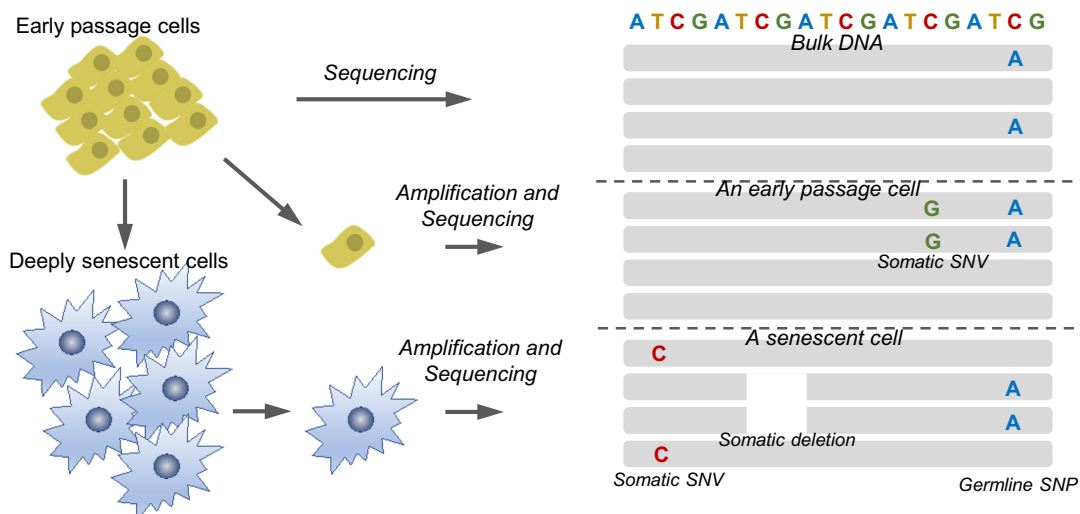


Figure 1. Schematic illustration of the detection of somatic mutations by single-cell whole-genome sequencing. Each track in gray presents a sequence read, and a dotted line separates reads of different samples. A, adenine; C, cytosine; G, guanine; T, thymine.

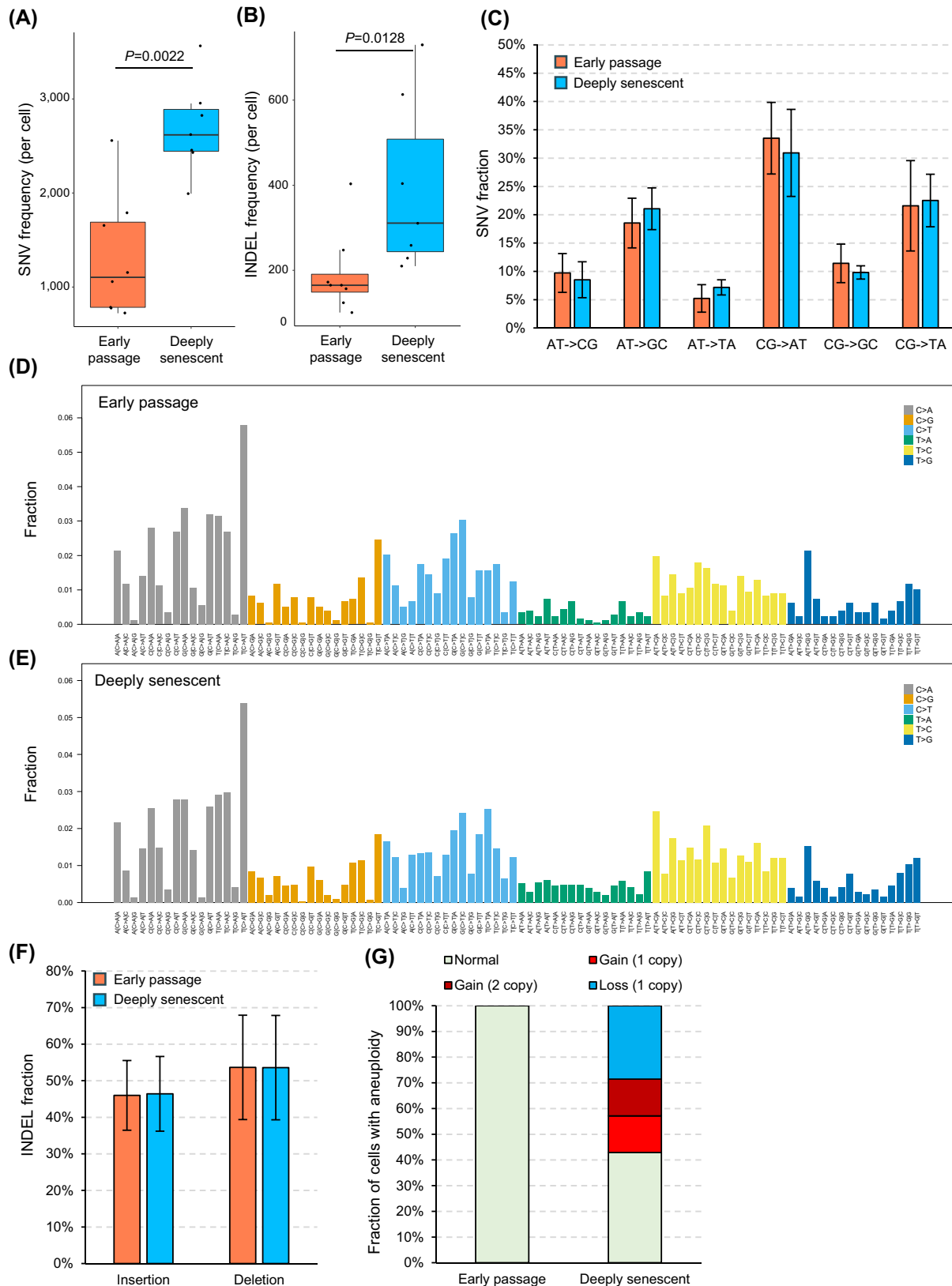


Figure 2. Somatic mutations in early passage and deeply senescent cells. (A) Single-nucleotide variant (SNV) and (B) small insertion and deletion (INDEL) frequencies. (C) SNV spectra. Refined SNV spectra by considering their flanking bases in (D) early passage and (E) senescent cells separately. (F) INDEL spectra. (G) Types of whole-chromosome aneuploidies. For panels (A and B), p values were estimated using the Wilcoxon Rank Sum test, two-tailed. Box plot elements are: center line, median; box limits, upper and lower quartiles; whiskers, 1.5× interquartile range; points, all data points. For panels (C) and (F), bars represent means and error bars standard deviations. A, adenine; C, cytosine; G, guanine; T, thymine.

increase in clonal development of mutations as cells approach senescence, and may be due to extensive cell passaging.

We also annotated the predicted effects of mutations in protein-coding sequences using wANNOVAR²⁴. Among the 65 non-synonymous or loss-of-function mutations observed, a stop codon mutation in the *SLC36A9* gene and a non-synonymous mutation in the *CCDC114* gene were notable (Table S3). Both mutations were observed in three out of the seven senescent cells analyzed, indicating that they have expanded to a significant fraction of the population prior to senescence.

Aneuploidies were only observed in senescent cells

We then identified aneuploidies in the single-cell sequencing data based on our recently developed read depth-based tool¹⁶. In early passage cells, we did not observe any whole-chromosome aneuploidy, although we found one large deletion on one copy of chromosome 2 in one of the eight cells (**Supplementary Figure 3**). In contrast, we observed that four of the seven senescent cells showed whole-chromosome gain or loss, including a 2-copy-gain of chr.18, a 1-copy-loss of chr.19, a 1-copy-gain and 1-copy-loss of chr.22 (**Fig. 2G** and **Supplementary Figure 4**). These results indicate that unlike smaller mutations (SNVs and INDELs), the rate of aneuploidies is significantly elevated in senescent cells as compared to early passage cells. Because senescent cells have permanently exited the cell cycle, this excessive aneuploidy is likely due to errors in the last mitotic replication before the cells become senescent. This finding of an increased frequency of aneuploidy in senescent cells is in agreement with previous findings of increased aneuploidy in human senescent fibroblasts²⁵ and suggests that aneuploidy accompanies the entry into senescence and could even be its driving cause²⁵. In view of the fact that senescent cells can be in G1 or G2 phase of the cell cycle, it would be of interest to study aneuploidy in relation to the cell cycle. Unfortunately, our single-cell whole-genome sequencing data did not readily allow us to do this, because based on sequencing depth alone, we cannot distinguish if a cell contains two copies or four copies of the genome.

Discussion

The role of somatic mutations as a cause of chronic conditions or diseases, such as cancer and aging, has been hypothesized since the 1950s¹. Soon afterward, mutations were indeed implicated as the cause of cancer²⁶. However, tumors are clonal and can be readily analyzed for somatic mutations. Most normal somatic tissues are not clonal and somatic mutation profiles are different from cell to cell, with the exception of a few clonally amplified mutations, such as in clonal hematopoiesis²⁷. With the development of methods based on single-cell sequencing or clonal outgrowth followed by sequencing, mutation accumulation has been discovered during human aging in all cell types analyzed^{3,5,7,28}. Mutation frequencies differ significantly by cell type, and can vary from a few hundred in newborns to several thousand per cell in elderly. Although some somatic mutations provide a growth advantage to cells, for example, in cancer or in clonal hematopoiesis²⁹, most mutations are either neutral or have adverse effects. Indeed, we previously found that in human B lymphocytes, most mutations in functional sequences were negatively selected during aging⁷.

In this study, we directly analyzed mutation frequencies and spectra in replicatively senescent human cells. The SNV and

INDEL frequencies of senescent cells significantly increased comparing to early passage cells and are in the same range of those observed in cells from elderly subjects³⁰. This suggests that the increase may be expected simply as a result of cell replication. However, it remains untested if increased SNV and INDEL frequencies alone can cause senescence. As observed in our recent study, SNV and INDEL frequencies of normal, human lung epithelial cells are positively associated with tobacco-smoking pack years, but the frequencies no longer increase in humans of approximately 20 or more pack years⁴. So, it remains to be tested if SNV and INDEL frequencies can further increase without severely damaging cellular function or leading to cell-fate changes.

Aneuploidy increases substantially more than expected based on the number of cell divisions. This makes it a potential cause of senescence because these aneuploidies likely have arisen during the cell divisions before senescence²⁵. As shown recently, cellular senescence can be driven by the presence of cytoplasmic chromatin fragments³¹. It is yet unclear if the whole-chromosomal loss (or gain) observed in senescent cells is a source of cytoplasmic DNA. Because cytoplasmic chromatin fragments associate with specific histone modifications, the above hypothesis may be addressed by applying single-cell chromatin immunoprecipitation sequencing in analyzing senescent cells³².

Overall, the above results provide the first evidence of somatic mutation accumulation in senescent cells. As mentioned, senescence is a comprehensive phenotype and can be a result of many different factors besides replication. It still requires future investigation whether the patterns and roles of mutations are the same or different in different types of senescent cells.

Experimental Procedures

IMR-90 fibroblasts were obtained from the ATCC (CCL-186) and cultured using physiological oxygen conditions (92.5% N₂, 5% CO₂, 2.5% O₂) as described³³. Cultures were serially propagated at 1:4 dilution at each passage (hence one passage is equivalent to two population doublings). After proliferation ceased (passage 38), the cultures were kept in the senescent state for 4–5 months with regular media changes as described³³. Single cells were isolated into individual PCR tubes using the CellRaft System (Cell Microsystems) according to manufacturer's instructions and kept at –80°C until amplification.

Single-cell whole-genome amplifications were performed using the SCMDA method¹⁵. In brief, 1 μL Exo-Resistant random primer (Thermo Fisher Scientific) and 3 μL lysis buffer (400 mM KOH, 100 mM DTT, and 10 mM EDTA) were added to the cell and kept on ice for 10 min. Then, 3 μL stop buffer (400 mM HCl and 600 mM Tris-HCl pH 7.5) was added for neutralization. Finally, 32 μL Master Mix containing 30 μL MDA reaction buffer and 2 μL Phi29 polymerase (REPLI-g UltraFast Mini Kit; Qiagen) were added. The amplification was performed at 30°C for 1.5 hours, 65°C for 3 min, and 4°C until purification. Purification was performed using AMPureXP-beads (Beckman Coulter). The final product was quantified using the Qubit High-Sensitivity dsDNA kit (Thermo Fisher Scientific). Bulk DNA was extracted from early passage fibroblasts using the Quick-DNA kit (Zymo Research).

Whole-genome sequencing libraries were prepared using the TruSeq Nano DNA HT Sample Prep Kit (Illumina), and sequenced on the Illumina HiSeq X Ten System with 2 × 150 bp paired-end reads by Novogene. After quality control and trimming using FastQC (v0.11.9) and Trim Galore (v0.6.4)^{34,35}, sequencing reads

were aligned to the human reference (Build 37) using BWA mem (v0.7.17)³⁶. PCR duplicates were removed using samtools (v1.9)³⁷. The alignment was INDEL-realigned and base pair recalibrated using GATK (v3.5.0)³⁸. Somatic SNVs and INDELS of a single cell were called using SCcaller (v2.0.0) requiring at least 20× sequencing depth and by comparing the single-cell data to the bulk DNA-seq data¹⁵. Somatic RTs were called using TraFiC-mem with default parameters³⁹. Large copy number variations and aneuploidies were identified using SCCNV (bin size: 500,000 bp; number of bins per window: 100; v1.0.2)¹⁶.

Acknowledgments

L.Z. is supported by the American Federation for Aging Research Grant (the Sagol Network GerOmic Award for Junior Faculty). X.D. is supported by the National Institutes of Health (NIH) R00 AG056656, P01 HL160476, U54 AG076041, and U54 AG079754. J.M.S. is supported by the NIH R01 AG016694 and P01 AG051449. J.V. is supported by the NIH P01 AG017242, P01 AG047200, and U01 ES029519.

Author Contributions

J.M.S. and J.V. conceived the study, L.Z., M.D.C., and M.L. performed experiments, X.D. and X.H. analyzed the data, and L.Z. and X.D. prepared this article with input from all coauthors.

Declaration of Interests

L.Z., X.D., M.L., A.Y.M., and J.V. are cofounders of SingulOmics Corp. J.M.S. and M.D.C. are named as coinventors on patents filed by Brown University and licensed to Transposon Therapeutics Inc. J.M.S. is a cofounder and SAB chair of Transposon Therapeutics and consults for Atropos Therapeutics, Gilead Sciences, and Oncolinea. The others declare no conflict of interest.

Data Availability Statement

Single-cell sequencing data are available at the NCBI dbGAP database under phs002610.v2.

Supplemental Information

Supplemental information can be found online at <https://doi.org/10.59368/agingbio.20230005>.

Accepted May 20, 2023

Published June 27, 2023

References

1. Failla G. (1958). The aging process and cancerogenesis. *Ann. N. Y. Acad. Sci.* **71**(6), 1124–1140. PMID: 13583876; doi: 10.1111/j.1749-6632.1958.tb46828.x.
2. Szilard L. (1959). On the nature of the aging process. *Proc. Natl. Acad. Sci. U. S. A.* **45**(1), 30–45. PMID: 16590351; doi: 10.1073/pnas.45.1.30.
3. Brazhnik K., Sun S., Alani O., ... Dong X., & Vijg J. (2020). Single-cell analysis reveals different age-related somatic mutation profiles between stem and differentiated cells in human liver. *Sci. Adv.* **6**(5), eaax2659. PMID: 32064334; doi: 10.1126/sciadv.aax2659.
4. Huang Z., Sun S., Lee M., ... Spivack S.D., & Vijg J. (2022). Single-cell analysis of somatic mutations in human bronchial epithelial cells in relation to aging and smoking. *Nat. Genet.* **54**(4), 492–498. PMID: 35410377; doi: 10.1038/s41588-022-01035-w.
5. Lodato M.A., Rodin R.E., Bohrsen C.L., ... Park P.J., & Walsh C.A. (2018). Aging and neurodegeneration are associated with increased mutations in single human neurons. *Science* **359**(6375), 555–559. PMID: 29217584; doi: 10.1126/science.aao4426.
6. Vijg J., & Dong X. (2020). Pathogenic mechanisms of somatic mutation and genome mosaicism in aging. *Cell* **182**(1), 12–23. PMID: 32649873; doi: 10.1016/j.cell.2020.06.024.
7. Zhang L., Dong X., Lee M., Maslov A.Y., Wang T., & Vijg J. (2019). Single-cell whole-genome sequencing reveals the functional landscape of somatic mutations in B lymphocytes across the human lifespan. *Proc. Natl. Acad. Sci. U. S. A.* **116**(18), 9014–9019. PMID: 30992375; doi: 10.1073/pnas.1902510116.
8. Gorgoulis V., Adams P.D., Alimonti A., ... Serrano M., & Demaria M. (2019). Cellular senescence: Defining a path forward. *Cell* **179**(4), 813–827. PMID: 31675495; doi: 10.1016/j.cell.2019.10.005.
9. Coppé J.P., Patil C.K., Rodier F., ... Desprez P.Y., & Campisi J. (2008). Senescence-associated secretory phenotypes reveal cell-nonautonomous functions of oncogenic RAS and the p53 tumor suppressor. *PLoS Biol.* **6**(12), 2853–2868. PMID: 19053174; doi: 10.1371/journal.pbio.0060301.
10. Pignolo R.J., Passos J.F., Khosla S., Tchkonja T., & Kirkland J.L. (2020). Reducing senescent cell burden in aging and disease. *Trends Mol. Med.* **26**(7), 630–638. PMID: 32589933; doi: 10.1016/j.molmed.2020.03.005.
11. Cruickshanks H.A., McBryan T., Nelson D.M., ... Berger S.L., & Adams P.D. (2013). Senescent cells harbour features of the cancer epigenome. *Nat. Cell Biol.* **15**(12), 1495–1506. PMID: 24270890; doi: 10.1038/ncb2879.
12. Correia-Melo C., Marques F.D., Anderson R., ... Korolchuk V.I., & Passos J.F. (2016). Mitochondria are required for pro-ageing features of the senescent phenotype. *Embo. J.* **35**(7), 724–742. PMID: 26848154; doi: 10.15252/embj.201592862.
13. Fumagalli M., Rossiello F., Clerici M., ... Longhese M.P., & d'Adda di Fagagna F. (2012). Telomeric DNA damage is irreparable and causes persistent DNA-damage-response activation. *Nat. Cell Biol.* **14**(4), 355–365. PMID: 22426077; doi: 10.1038/ncb2466.
14. Campisi J. (2013). Aging, cellular senescence, and cancer. *Annu. Rev. Physiol.* **75**, 685–705. PMID: 23140366; doi: 10.1146/annurev-physiol-030212-183653.
15. Dong X., Zhang L., Milholland B., ... Wang T., & Vijg J. (2017). Accurate identification of single-nucleotide variants in whole-genome-amplified single cells. *Nat. Methods* **14**(5), 491–493. PMID: 28319112; doi: 10.1038/nmeth.4227.
16. Dong X., Zhang L., Hao X., Wang T., & Vijg J. (2020). SCCNV: A software tool for identifying copy number variation from single-cell whole-genome sequencing. *Front Genet.* **11**, 505441. PMID: 33304377; doi: 10.3389/fgene.2020.505441.
17. Preston B.D., Albertson T.M., & Herr A.J. (2010). DNA replication fidelity and cancer. *Semin. Cancer Biol.* **20**(5), 281–293. PMID: 20951805; doi: 10.1016/j.semcancer.2010.10.009.
18. Alexandrov L.B., Kim J., Haradhvala N.J., ... Rozen S.G., & Stratton M.R. (2020). The repertoire of mutational signatures in human cancer. *Nature* **578**(7793), 94–101. PMID: 32025018; doi: 10.1038/s41586-020-1943-3.
19. Gel B., & Serra E. (2017). karyoploteR: An R/Bioconductor package to plot customizable genomes displaying arbitrary data. *Bioinformatics* **33**(19), 3088–3090. PMID: 28575171; doi: 10.1093/bioinformatics/btx346.
20. Wang J., Gonzalez K.D., Scaringe W.A., ... Hill K.A., & Sommer S.S. (2007). Evidence for mutation showers. *Proc. Natl. Acad. Sci. U. S. A.* **104**(20), 8403–8408. PMID: 17485671; doi: 10.1073/pnas.0610902104.
21. Lora D. (2016). ClusteredMutations: Location and visualization of clustered somatic mutations. <https://cran.r-project.org/web/packages/ClusteredMutations/index.html>.
22. Greaves M., & Maley C.C. (2012). Clonal evolution in cancer. *Nature* **481**(7381), 306–313. PMID: 22258609; doi: 10.1038/nature10762.

23. Jaiswal S., & Ebert B.L. (2019). Clonal hematopoiesis in human aging and disease. *Science* **366**(6465). PMID: [31672865](#); doi: [10.1126/science.aan4673](#).
24. Chang X., & Wang K. (2012). wANNOVAR: Annotating genetic variants for personal genomes via the web. *J. Med. Genet.* **49**(7), 433–436. PMID: [22717648](#); doi: [10.1136/jmedgenet-2012-100918](#).
25. Andriani G.A., Almeida V.P., Faggioli F., ... Vijg J., & Montagna C. (2016). Whole chromosome instability induces senescence and promotes SASP. *Sci Rep.* **6**, 35218. PMID: [27731420](#); doi: [10.1038/srep35218](#).
26. Nowell P.C. (1976). The clonal evolution of tumor cell populations. *Science* **194**(4260), 23–28. PMID: [959840](#); doi: [10.1126/science.959840](#).
27. Jaiswal S., Fontanillas P., Flannick J., ... Altshuler D., & Ebert B.L. (2014). Age-related clonal hematopoiesis associated with adverse outcomes. *N. Engl. J. Med.* **371**(26), 2488–2498. PMID: [25426837](#); doi: [10.1056/NEJMoa1408617](#).
28. Blokzijl F., de Ligt J., Jager M., ... Cuppen E., & van Boxtel R. (2016). Tissue-specific mutation accumulation in human adult stem cells during life. *Nature* **538**(7624), 260–264. PMID: [27698416](#); doi: [10.1038/nature19768](#).
29. Zink F., Stacey S.N., Norddahl G.L., ... Kong A., & Stefansson K. (2017). Clonal hematopoiesis, with and without candidate driver mutations, is common in the elderly. *Blood* **130**(6), 742–752. PMID: [28483762](#); doi: [10.1182/blood-2017-02-769869](#).
30. Ren P., Dong X., & Vijg J. (2022). Age-related somatic mutation burden in human tissues. *Front Aging* **3**, 1018119. PMID: [36213345](#); doi: [10.3389/fragi.2022.1018119](#).
31. Miller K.N., Victorelli S.G., Salmonowicz H., ... Passos J.F., & Adams P.D. (2021). Cytoplasmic DNA: Sources, sensing, and role in aging and disease. *Cell* **184**(22), 5506–5526. PMID: [34715021](#); doi: [10.1016/j.cell.2021.09.034](#).
32. Rotem A., Ram O., Shores N., ... Weitz D.A., & Bernstein B.E. (2015). Single-cell ChIP-seq reveals cell subpopulations defined by chromatin state. *Nat. Biotechnol.* **33**(11), 1165–1172. PMID: [26458175](#); doi: [10.1038/nbt.3383](#).
33. De Cecco M., Ito T., Petrashen A.P., ... Neretti N., & Sedivy J.M. (2019). L1 drives IFN in senescent cells and promotes age-associated inflammation. *Nature* **566**(7742), 73–78. PMID: [30728521](#); doi: [10.1038/s41586-018-0784-9](#).
34. Gossen J.A., de Leeuw W.J., Tan C.H., ... Knook D.L., & Vijg J. (1989). Efficient rescue of integrated shuttle vectors from transgenic mice: A model for studying mutations in vivo. *Proc. Natl. Acad. Sci. U. S. A.* **86**(20), 7971–7975. PMID: [2530578](#); doi: [10.1073/pnas.86.20.7971](#).
35. Kong A., Frigge M.L., Masson G., ... Thorsteinsdottir U., & Stefansson K. (2012). Rate of de novo mutations and the importance of father's age to disease risk. *Nature* **488**(7412), 471–475. PMID: [22914163](#); doi: [10.1038/nature11396](#).
36. Li H. (2013). Aligning sequence reads, clone sequences and assembly contigs with BWA-MEM. arXiv preprint. [arXiv:1303.3997](#).
37. Li H., Handsaker B., Wysoker A., ... Durbin R., & Genome Project Data Processing S. (2009). The sequence alignment/map format and SAMtools. *Bioinformatics* **25**(16), 2078–2079. PMID: [19505943](#); doi: [10.1093/bioinformatics/btp352](#).
38. McKenna A., Hanna M., Banks E., ... Daly M., & DePristo M.A. (2010). The genome analysis toolkit: A MapReduce framework for analyzing next-generation DNA sequencing data. *Genome Res.* **20**(9), 1297–1303. PMID: [20644199](#); doi: [10.1101/gr.107524.110](#).
39. Rodriguez-Martin B., Alvarez E.G., Baez-Ortega A., ... Campbell P.J., & Tubio J.M.C. (2020). Pan-cancer analysis of whole genomes identifies driver rearrangements promoted by LINE-1 retrotransposition. *Nat. Genet.* **52**(3), 306–319. PMID: [32024998](#); doi: [10.1038/s41588-019-0562-0](#).